Faculty of Mechatronics and interdisciplinary engineering studies

Student's Project

Supervisors: Dr Bernd Dehning, ing Jan Koopman (CERN)

Tutor: Doc. RNDr. Miroslav Šulc, Ph.D. (TUL)

Measurement and optical design for Beam Ionization Profile Monitor in CERN SPS

Daniel KRAMER

Contents

Annotation

Measurement, development and optical design for Beam Ionization Profile Monitor in Super Proton Synchrotron were a part of the 12 moths working period spent in Beam Diagnostics and Instrumentation group (AB/BDI/BL) in CERN. IPM principally detects electrons produced by ionization of nitrogen gas and delivers a beam profile thanks to electron-photon conversion and CCD imaging.

The aim was to determine whether the IPM was able to measure with expected accuracy and repeatability in continuous mode the proton beam vertical emittance under different energy and intensity conditions planned for future Large Hadron Collider.

Several improvements were made during the 2003 run and an offline data analysis (via Matlab files) was implemented. Thanks to the measurements, various problems were discovered and should be eliminated in the next generation IPM.

Measurements showed a good reproducibility and confirmed the satisfying dynamic range of the instrument.

Optical design was made in Zemax program for the new IPM with two optical paths. Two standard doublets and a custom designed 3-element objective were used. Mounted system is being tested.

Anotace

Měření, vývoj a optický design pro Beam Ionization Profile Monitor (IPM) v SPS byli součástí pracovní stáže strávené ve skupině AB/BDI/BL v CERN.

IPM detekuje elektrony tvořené ionizací plynu a zobrazuje profil svazku díky elektron-fotonové konverzi a CCD kameře.

Cílem bylo zjistit, jestli je IPM schopný měřit s požadovanou přesností a reprodukovatelností vertikální emittanci při různých intenzitách a energiích svazku plánovaných pro budoucí urychlovač LHC.

Během roku 2003 byla provedena některá vylepšení a zavedena offline analýza dat (v Matlabu). Měření odhalila různé problémy, které budou odstraněny v příští generaci detektoru. Byla prokázána dobrá reprodukovatelnost a dostatečný dynamický rozsah přístroje.

Optický návrh pro IPM se dvěmi větvemi byl proveden v programu Zemax. Byly použity 2 standardní dublety a 3 členný zakázkový objektiv. Soustava se nyní testuje.

1. Introduction

1.1. CERN and Technical Student Program

"The Technical Student Programme in Engineering, Computing and Applied Science

CERN Technical Student Programme is aimed at undergraduate students in technical fields, whose universities require or encourage them to spend a training period of several months during the course of their studies in industry or in a research establishment, or allow them to carry out a project in such an establishment. Selected students join a team working at CERN, and usually spend six to twelve months at the laboratory." (*Official CERN website)*

Student writing this report have spent 12 months in AB / BDI / BL (Accelerator Beams division / Beam Diagnostics and Instrumentation group / Beam Loss section). He was working in the exciting domain of applied physics for accelerator instrumentation.

CERN (European Center for Nuclear Research) is situated partially in Switzerland (close to Geneva) and France (Pays de Gex). It is one of the biggest research centers in the world and its primary concern is particle physics research. Particle accelerators are therefore being a heart of the center, because they are delivering particles for experiments. Now, the biggest accelerator in the world, in terms of energy and size, is being built in CERN. It is called LHC (Large Hadron Collider).

1.2. Ionization Profile Monitor (IPM)

Accelerators need for proper commissioning various beam diagnostics systems to show to its operators "what happens with the particles". IPM is one of the continuous operation detectors envisaged for implementation in LHC. Two prototypes are already installed in SPS (Super Proton Synchrotron) which should serve as a particle injector for LHC in the future.

IPM (Rest Gas Ionization Beam Profile Monitor) delivers a two dimensional beam projection in either horizontal or vertical plane. From these data and other accelerator parameters one is able to calculate the beam Emittance, a very important quality parameter characterizing each particle beam.

2. Accelerators background

2.1. Introduction to accelerators in CERN

High-energy circular particle accelerators have to be accompanied by a chain of smaller preceding acceleration units, because each one has an upper and lower energy limit. These ones are due mainly to magnet parameters and vacuum pipe dimensions. CERN accelerator chain consists of a particle source followed by an accelerating RFQ (radio frequency cavity), LINAC (linear accelerator), BOOSTER (circular accelerator with 4 parallel pipes), PS (proton synchrotron), SPS (super proton synchrotron) and finally the superconducting LHC (large hadron collider) under construction. Highly relativistic particles are injected into SPS for fixed target operation with energy of 14 GeV than ramped to 400 GeV and extracted towards experimental areas. Test beams used for LHC operation are received at 26 GeV and extracted towards LHC at 450 GeV. LHC will be able to reach 7 TeV per proton. Particles are circulating in so-called bunches, because a periodic RF acceleration field is applied. Their length corresponds to half the wavelength of the field. Nominal bunch spacing for LHC operation is 25ns or 75ns for the early stage of future commissioning (other parameters - see attachments). Bunches are grouped into Batches by 72 (corresponds to the full PS machine) and SPS can contain 4 Batches (also called injections).

CERN SPS machine and the future LHC is a partially circular synchrotron hadronic machine with separated function magnets.

Circular sections periodic lattice is composed of strong focusing and defocusing quadrupole magnets with bending dipole magnets in between them. This structure is called a FoDo cell and its function is to keep particles oscillating around a closed orbit inside the vacuum pipe. Sextupole and octupole magnets are inserted in the lattice to correct the imperfections of the FoDo cells.

Between the bended parts, there are straight sections with focusing magnets and places for either injection, extraction systems, acceleration cavities or beam instrumentation systems. In most of the straight sections, the radiation is lower and the electronics suffers less.

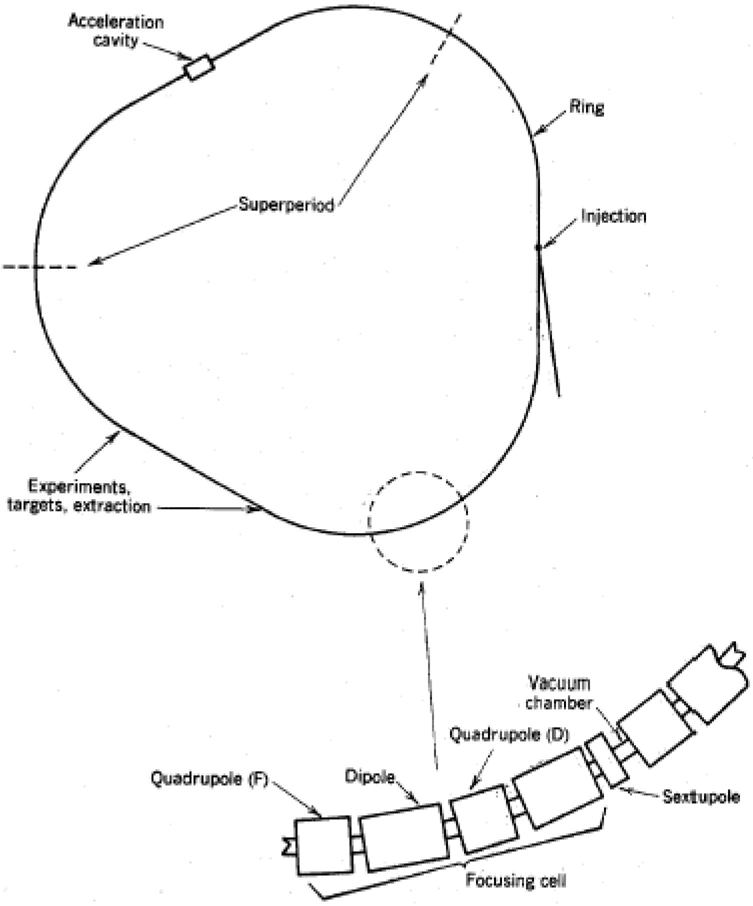

Figure 15.14 Major components and definition of terms in separated function synchrotron.

Stanley Humphries Jr.1999

2.2. Phase space

First, we have to introduce a coordinate system to describe easily the movement of each particle. Let s be the longitudinal (along the beam pipe), x horizontal transverse and y vertical transverse coordinate. The system is moving along the ideal close orbit trajectory. Than the particle's movement in our system can be described by the Hill's equation:

$$\frac{d^2x}{ds^2} + K(s)x = 0$$

It is in fact an equation of a simple harmonic motion. Where K is a restoring force caused by magnetic fields of the lattice.

It can be simply shown, that u(s) solves this equation.

$$u(s) = \sqrt{\varepsilon}\sqrt{\beta(s)}\cos(\psi(s) - \psi_0)$$

Where u(s) can be either x or y and ψ is a phase advance of the quasi-periodic motion. β(s) is called the betatron function and it determines the amplitude modulation due to changing focusing strength.

The derivative of u(s) is

$$u'(s) = -\alpha\sqrt{\frac{\varepsilon}{\beta}}\cos(\psi - \psi_0) - \sqrt{\frac{\varepsilon}{\beta}}\sin(\psi - \psi_0)$$

Where $\alpha = -\beta'/2$

If we eliminate the phase ψ, we obtain the constant of motion called Courant – Snyder invariant:

$$\gamma u^2 + 2\alpha u u' + \beta u'^2 = \varepsilon$$

Where $\gamma = \frac{1+\alpha^2}{\beta}$

This is in fact equation of an ellipse in a Phase space with horizontal axis u end vertical u'.

Movement of a particle in the synchrotron is described by a corresponding point in the six dimensional phase space (x,p_x,y,p_y,s,E), where $p_x \approx p_0 x'$, $p_y \approx p_0 y'$ are the transverse momenta ($cp_0=\beta E_0$). E is the particle energy. Using the paraxial approximation $\sin(x') \approx x'$ with x' being the trajectory slope and considering no coupling between the horizontal and vertical movement, one can divide the phase space into three independent two dimensional Phase planes. We still consider energy E constant.

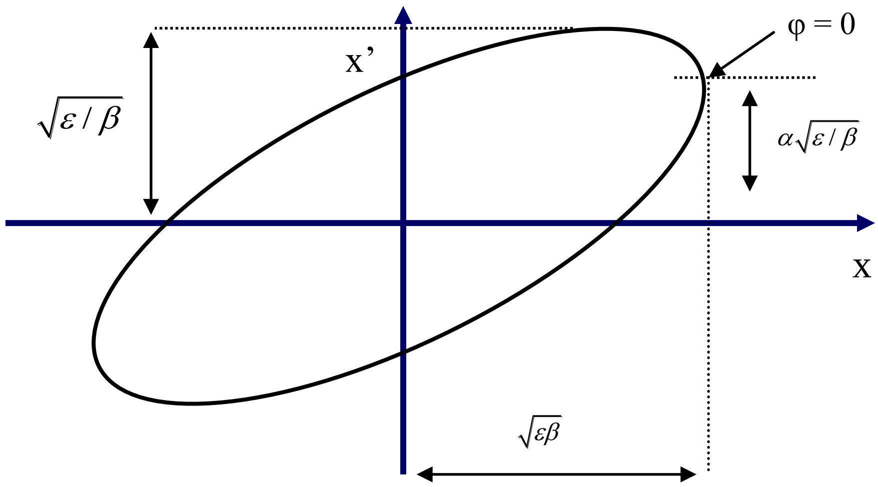

Phase plane ellipse with area πε and transverse coordinate x

2.3. Emittance

Physical interpretation of our invariant is that single particle will follow a 'trajectory' along the contour of the phase space (plane) ellipse. Parameters of the ellipse (α,β,γ) are changing along the beam line, so the orientation and dimensions are changing too.

It is not practical to count the trajectory for each particle. We generally want to describe the beam by its collective behavior.

Liouville's theorem tells us that the density of particles in phase space remains constant under the influence of conservative forces (without stochastic processes).

Thus if we find a particle with the highest amplitude and its phase ellipse, we know that all other ones are remaining inside it.

If we write for the argument in u(s)

$$\cos(\psi - \psi_0) = \pm 1$$

We get the beam envelope

$$E(s) = \pm\sqrt{\varepsilon}\sqrt{\beta(s)}$$

ε is called beam **Emittance** and is a major characteristic of the particle source. It can be viewed as a 'transverse temperature' of the beam (the same could be defined for longitudinal phase plane).
It is usually expressed in [mm mrad] or just in [μm].
While moving around the accelerator the shape of the ellipse changes because of β but its area πε remains constant.

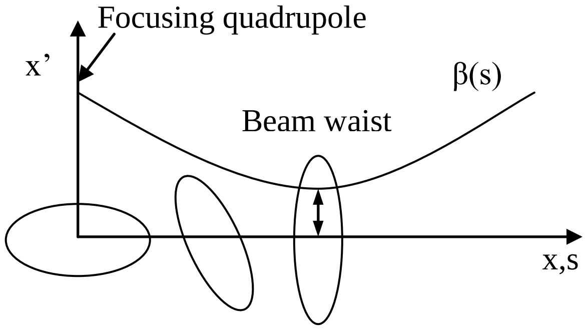

As it was already said, ε remains constant along the accelerator but with the condition, that also E stays constant. While accelerating the particles, one has to define a new invariant – Normalized Emittance:

$$\varepsilon_n = \beta\gamma\varepsilon$$

Where β = v/c and $\gamma = E/E_0$
One usually expects a Gaussian distribution inside the ellipse and particles relatively far from the central region as not important.
Thus, ε_n is usually defined as the Normalized Emittance at 1σ from the beam center.
In practice at high energies, one can usually measure only the distribution of particles in horizontal or vertical projection.
If we do not consider our beam as monochromatic (all particles with the same energy), a Dispersion term contributes to the measured σ_{meas}.

$$\sigma_{meas}^2 = \sigma_{emitt}^2 + \sigma_{disp}^2 = \beta\varepsilon + \left(D\frac{dp}{p} \right)^2$$

Where β as the betatron function and D as the dispersion function are the lattice parameters and can be found via lattice simulation programs. dp is the momentum spread inside the beam. Dispersion was not considered in the analysis, because IPM was in the low dispersion region and the perturbation was not important.

Than

$$\varepsilon = \frac{1}{(\beta)_{lattice}}\left[\sigma_{meas}^2 - \left(D\frac{dp}{p}\right)^2\right]$$

Finally the Normalized Emittance is:

$$\varepsilon_n = (\beta\gamma)_{beam}\,\varepsilon = \frac{(\beta\gamma)_{beam}}{(\beta)_{lattice}}\left[\sigma_{meas}^2 - \left(D\frac{dp}{p}\right)^2\right]$$

In this report, β_{beam} will be taken as 1, because only highly relativistic particles are considered.

Projection of the ellipse to its x-axis is the Physical transverse beam size.

3. Measurements with IPM

3.1. IPM detector description

The Ionization Profile Monitor is a continuous operation detector using the residual gas in the accelerator vacuum beam pipe as an “interaction medium”.

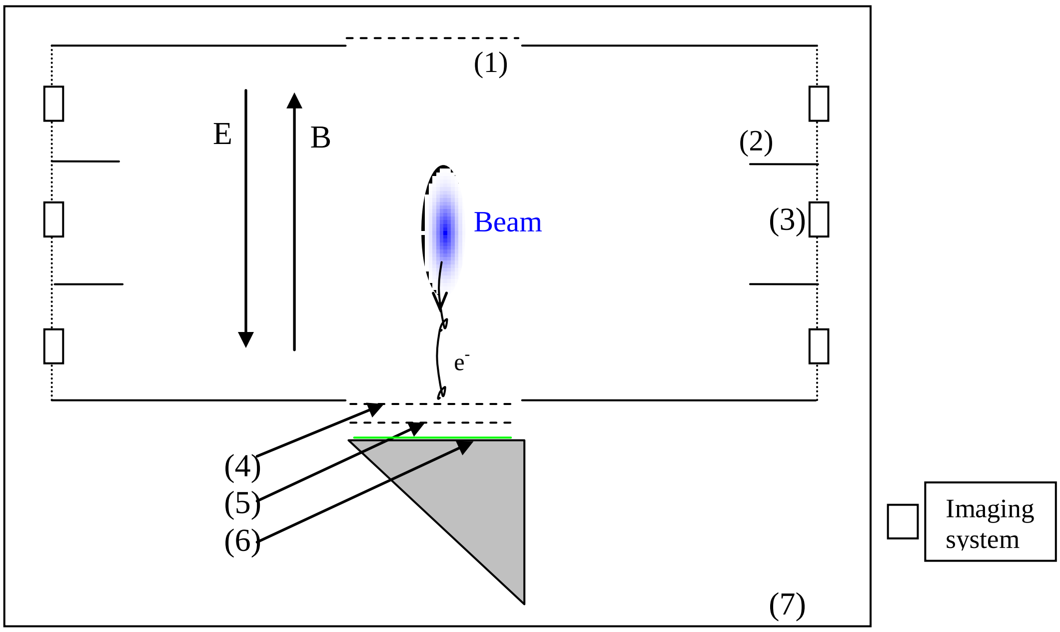

IPM detector schema (Image 3.1.)

(1)…Cathode grid

(2)…Field homogenization electrodes

(3)…Resistors

(4)…Multi-Channel Plate (MCP_{in}) entrance electrode

(5)…MCP_{out} exit electrode

(6)…Phosphor plate deposited on constantan and fused silica optical prism

(7)…Vacuum tank

Particle beam (perpendicular to the image) interacts with the rest gas (approx. 10^{-8} mbar) in the vacuum chamber, mostly with N_2 molecules. Electron can be detached from the nitrogen and than accelerated in the electric field towards the MCP_{in} electrode. Positive N_2^+ ions will travel on the opposite side through the cathode grid. Dipole magnetic field inside the tank forces the electrons to spiral around its field lines with a very small Larmor radius, because B = 0.1T and initial kinetic energy is around 10eV. Electrons are then multiplied (cca 10000 times) in the chevron type two-stage MCP. Between MCP_{out} and Phosphor plate is another high voltage applied, because the electrons exiting the MCP have a small energy. After the acceleration, electrons finish their path on the phosphor layer during the electron / photon conversion. Photons are reflected on the prism and detected in the imaging system behind a vacuum window.

3.2. IPM Data Acquisition System

Beam projection image formed on the phosphor plate is detected by an analog CCD camera with a standard CCIR TV resolution. Video signal is transmitted from the underground tunnel via a long (cca 200m) cable and digitized by a custom designed video card. Acquired data are stored in the acquisition computer memory and can be sent to a remote console or accessed by a Java application called BiScoTo.

There are two acquisition modes – Profiles and Images.

Each image is made from odd or pair lines and maximum repetition rate is around 1Hz.

Profiles are made by summing half-image lines. Cca 65 profiles can be made 'in a row' during one acquisition depending on the acquisition window size and corresponding memory limit. When the maximum profile repetition rate is set, it takes 40ms to get each profile, because every image is acquired for 20ms and then processed (summing the lines) for another 20ms.

Final data are stored in the asci format with a header containing various parameters.

3.3.Matlab programs for data processing

Profiles data were usually fitted directly in the Biscoto program and then the offline analysis was done through Matlab programs. Input to the created functions was mainly a text file containing all filenames of the desired acquisitions. Image files were fitted directly by Matlab programs. We implemented an image correction method, because the intensifier in IPM was perturbed by the stray B field and images were tilted.

3.4. Machine Developments (MD) at SPS 2003

EXPERIMENTAL RESULTS

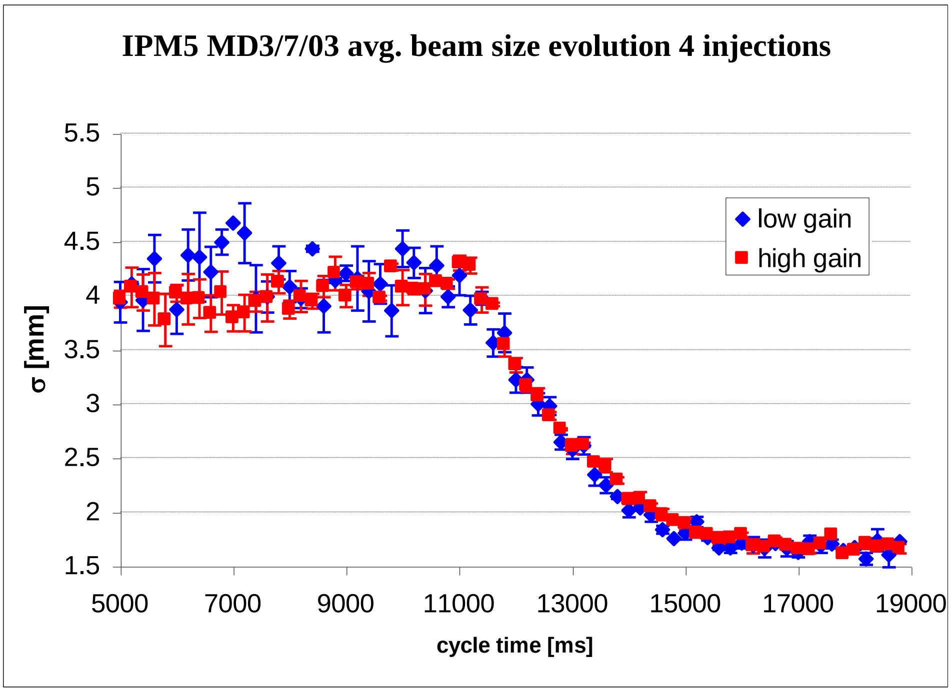

Beam size evolution independent on MCP gain or beam current Plot 3.2

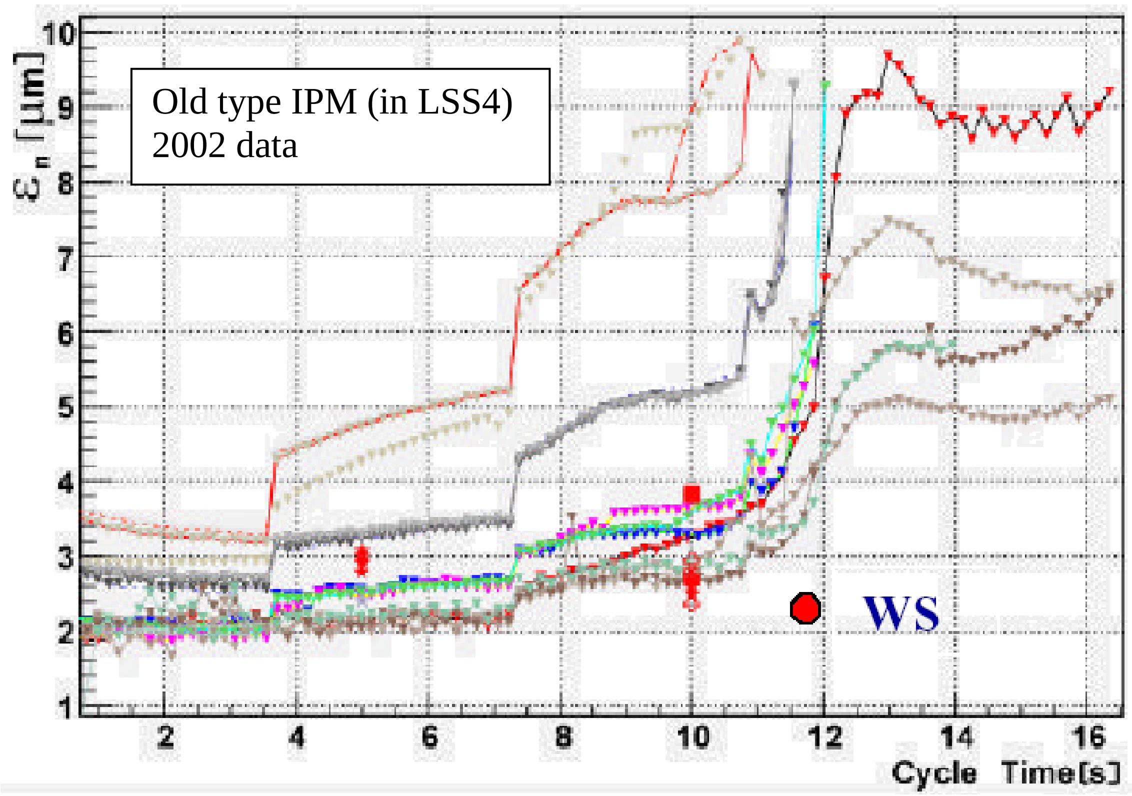

Beam emittance strongly dependent on MCP gain and changing with each injection Plot 3.3

Some major improvements were done on the IPM in LSS5 (Long Straight Section 5 in SPS) before starting of the 2003 run. For example, the NEG (Non-Evaporable electron Gutter: TiZrV: 15/34/51%) coating was applied on all surfaces "seeing the beam" to prevent the electron cloud build up (decreases the Secondary Electron Yield). Two-stage chevron type MCP was installed to increase the system sensitivity.

Effect of these improvements is illustrated by the **plots 3.2** and **3.3**. Measured sigma of the beam stays within a small range after all injections and is not sensitive to the gain change.
Nevertheless, we expect (for emittance conservation confirmed by the reference Wire Scanner profile monitor) the size shrinking factor 4.2 between low and high-energy beam, but observe cca 2.3. This was later improved by better focalization of the camera and closing the diaphragm of the camera lens by one stop.
(Beam momentum evolution is in attachments)

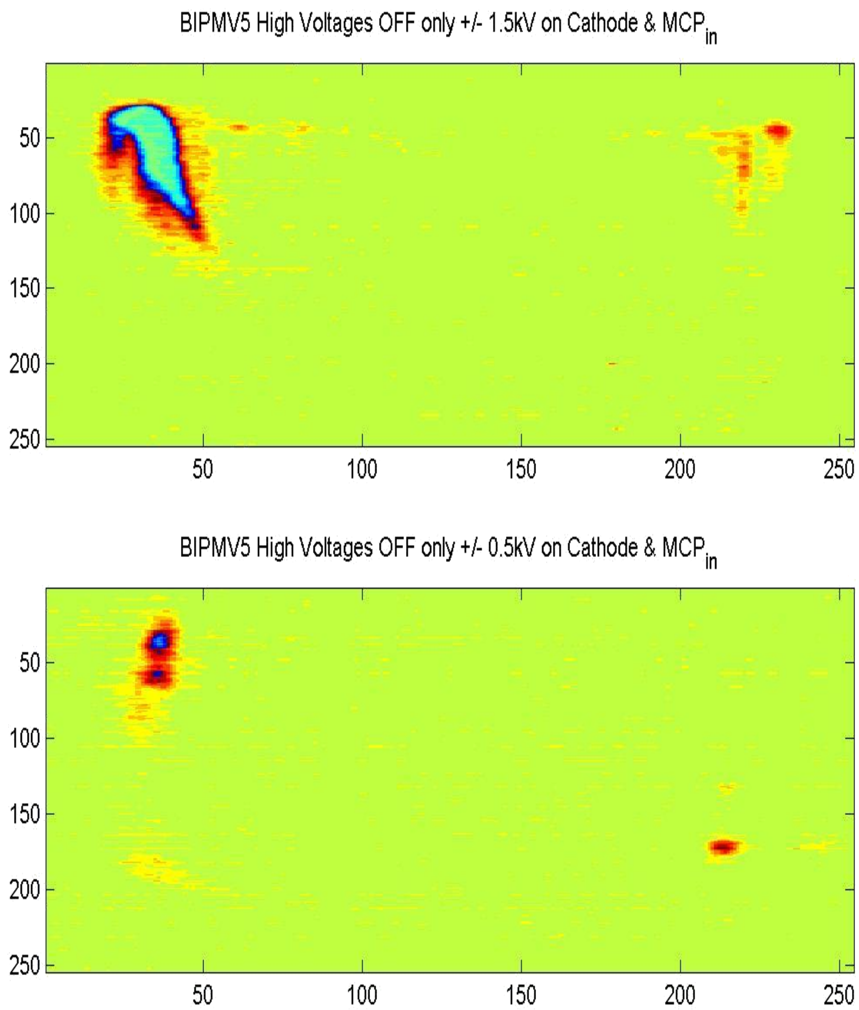

Electron jets coming to the phosphor plate due to the coupled high frequency EM oscillations from the beam *Image 3.4*

Full intensity LHC beam was tested during the 31/7/2003 MD.
One could see some high intensity flashes at high energy in IPM. They started to appear before the flat top. With 4-batches beam, some intensive spots appeared at flat top even without high voltages on! This was dependent only on the voltage applied between cathode and MCP_{in}. Spots were coming from the edges of the phosphor plate. **Images (3.4)** were taken at 18s of cycle time (≈450GeV).
These effects were found to be caused by the electromagnetic coupling between the beam and IPM electrodes while the very short bunches were used (~2ns). Collected weaves were than reflected by the resistors placed just after the high voltage connectors of the tank.

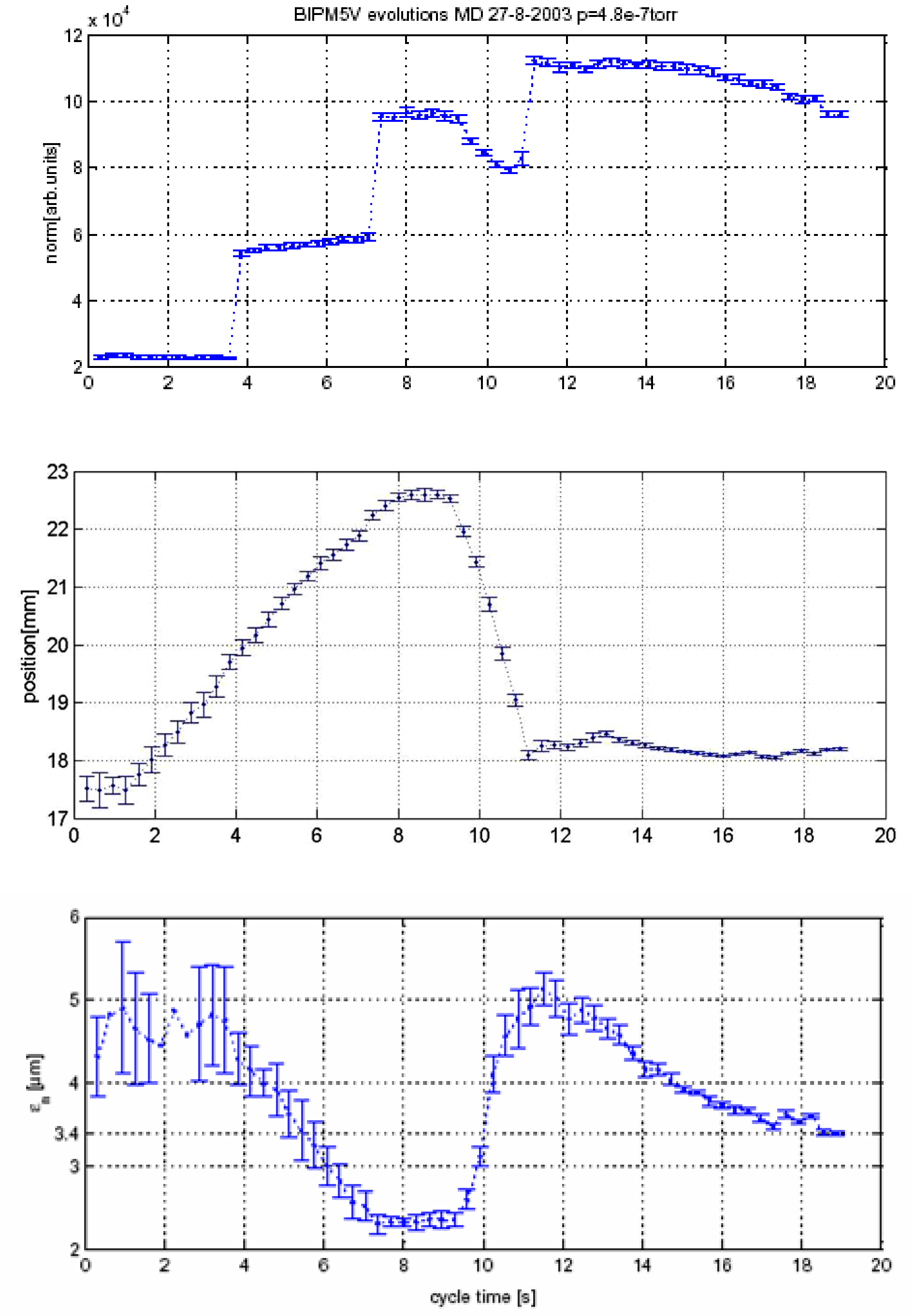

Discovered dependence of normalized emittance on beam position Plot 3.5

We finally managed to dump the coupled oscillations by placing the resistors right next to the high-voltage power supply in the surface building. Thou, the capacity of the whole cable was implied and helped to filter the very high frequencies.

After this success, we were able to measure in the whole dynamic range of SPS's proton currents and energies.

A programmed beam orbit bump helped us to show the non-homogeneity of the MCP active area. One can se on the plots 3.5 that normalized emittance varies and is correlated with beam position (Orbit bump was stopped at 11s – end of Flat Bottom).

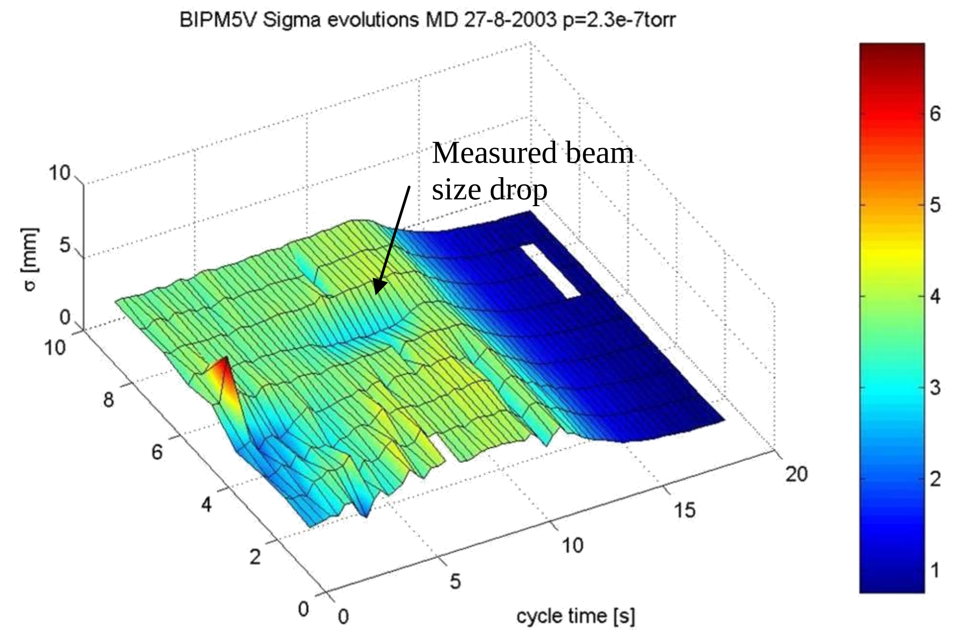

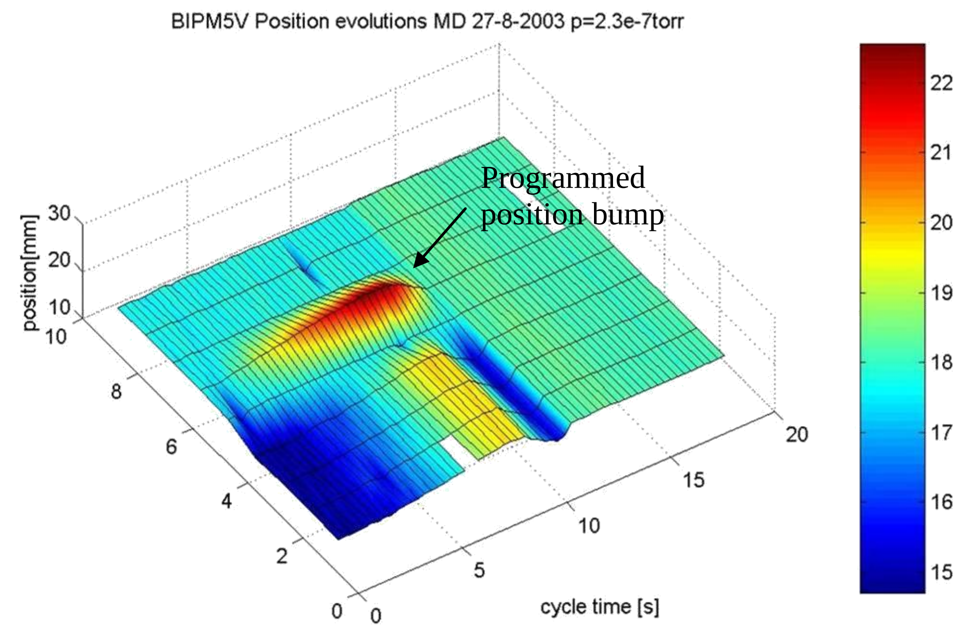

Time evolution of the beam movement and its influence on the measured beam size Plot 3.6

The **plot 3.6** shows the bump shape evolving with time (arbitrary units). Acquisition with arrow is also on the **plot 3.5**. Plotted 'Norm' is a sum of all CCD pixel values of each profile and approximately shows the measured beam intensity.

One can see the norm of the fits decreasing (1) after 1st injection and growing (3) after the injection of a 3rd batch (**plot 3.7**). This could be caused by a pressure increase after injection followed by a NEG coating gas sorption and by the electron cloud build up with 3 batches. During acceleration (4), the norm is slightly decreasing, which means we are loosing particles in the beam or the MCP is saturated and while the beam shrinks, it can't give more signal. Signal with 2 batches (2) seems stable.

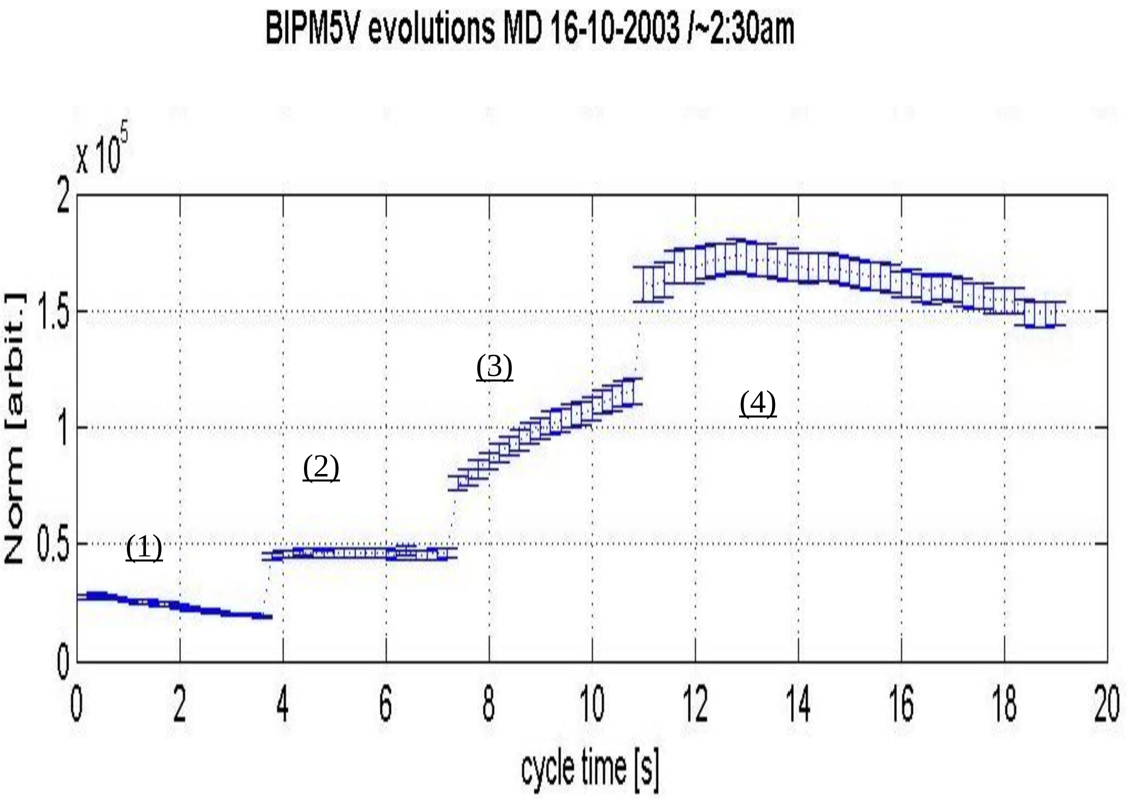

Evolution of number of electrons hitting the phosphor plate in arbitrary units during a cycle with 4 injections and acceleration *Plot 3.7*

Fixed pattern noise was subtracted from image projections and the resulting data were fitted by a Matlab file (**Plot 3.8**). The noise was measured previously during a period without beam. 64 profile evolutions were stored, each one including 94 profiles. Than an average of all these profiles was made. To be able to subtract this average it is necessary to use always the same acquisition window. Problem could occur if the noise pattern was measured on odd image frame acquisitions and data measured from even frames (and vice versa).

Another proposed method is to store profile evolutions with at least 2 profiles after beam dump to have a noise acquisition corresponding to the same frame parity because it is generally not known what parity we use. Profiles in the same acquisition sequence have the same parity.

The SNR is arbitrarily defined here as the fit amplitude / fit offset. This value can be used only for comparison.

The normalized emittance seems to be conserved. This needs to be compared with wire scanners. Image projections were fitted (Gaussian profile) with Matlab LAR method.

After fixed pattern noise subtraction, the fitted offset decreased from cca 250 to cca 60 units of intensity. In this way, we increased the "S/N" ratio.

The offset level grows with intensity and mainly with energy. This simply means that there is a growing radiation during the cycle in the tunnel.

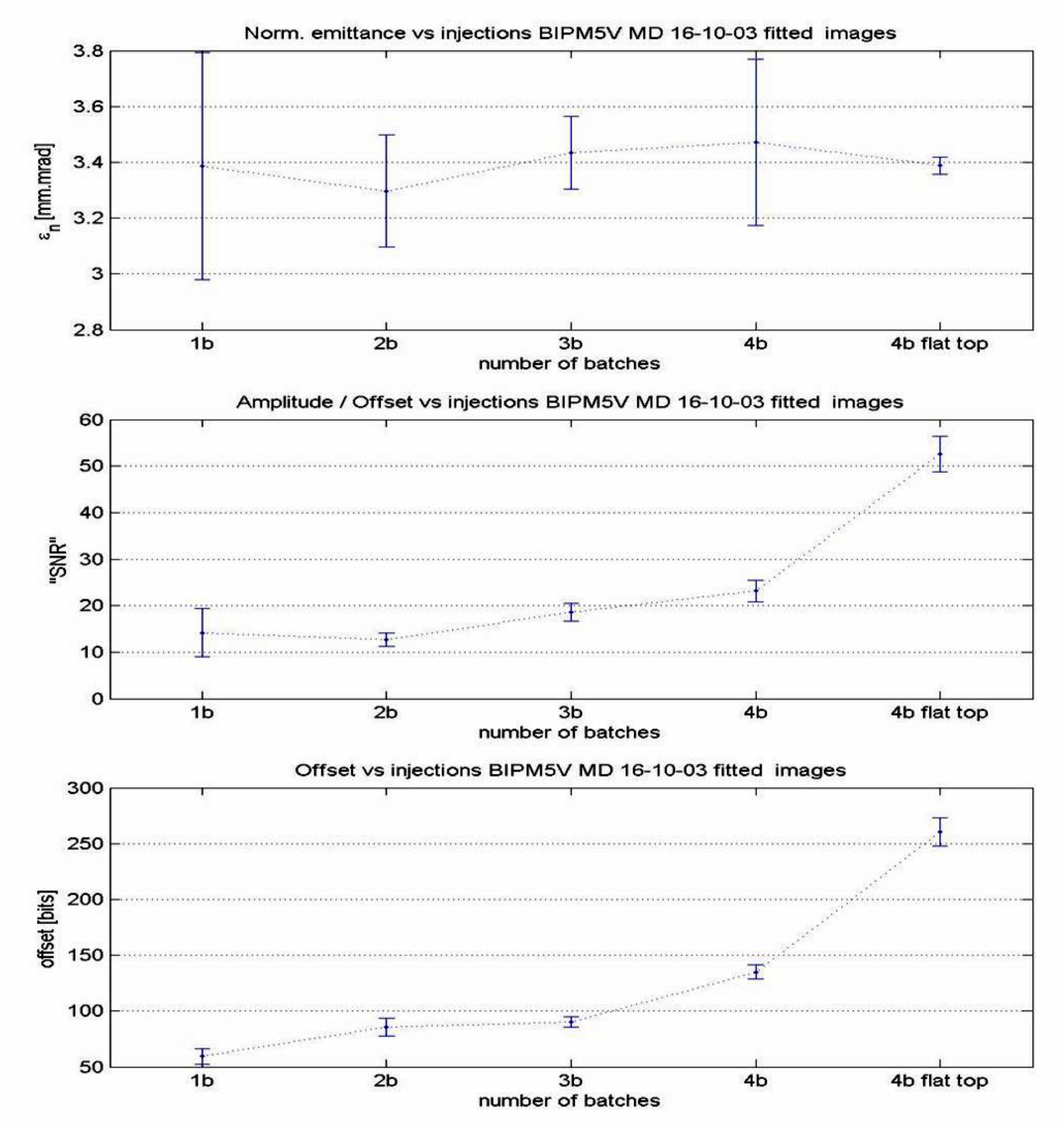

Fitted beam image projections after the fixed pattern noise subtraction and resulting arbitrary defined SNR. *Plot 3.8*

Plot 3.9 is an example of a fixed pattern noise correction (caused by CCD irradiation) One can see that the fitted amplitude increased by 3% while the size decreased by 7%. Anyway, that time we expected a beam size much smaller (cca 1.35bins – pilot bunch see MD11/11) to match the wire scanner data. The resolution limitation is believed to be the limited bandwidth of our video transmission line together with optical resolution. The profile was made by summing the lines of the image below.

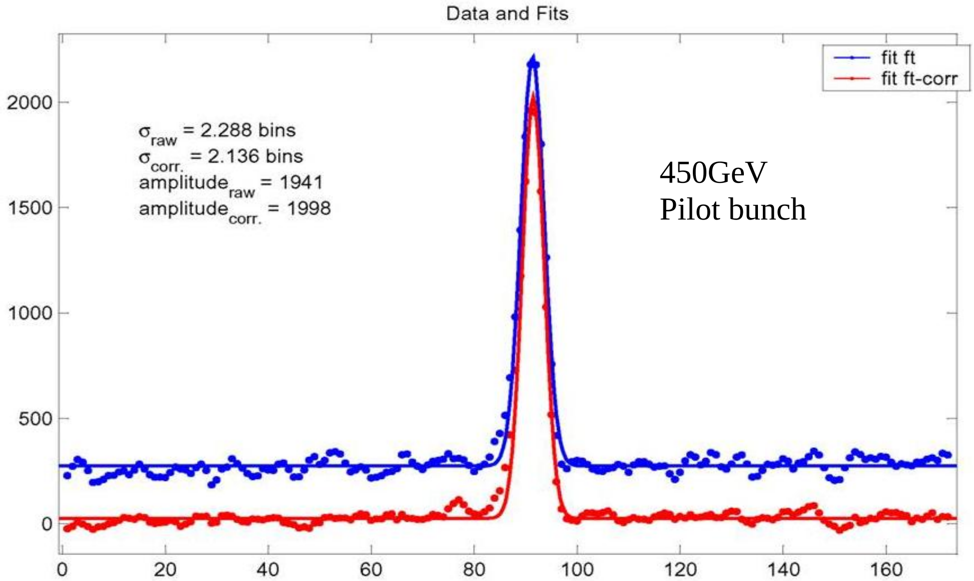

Plot 3.9

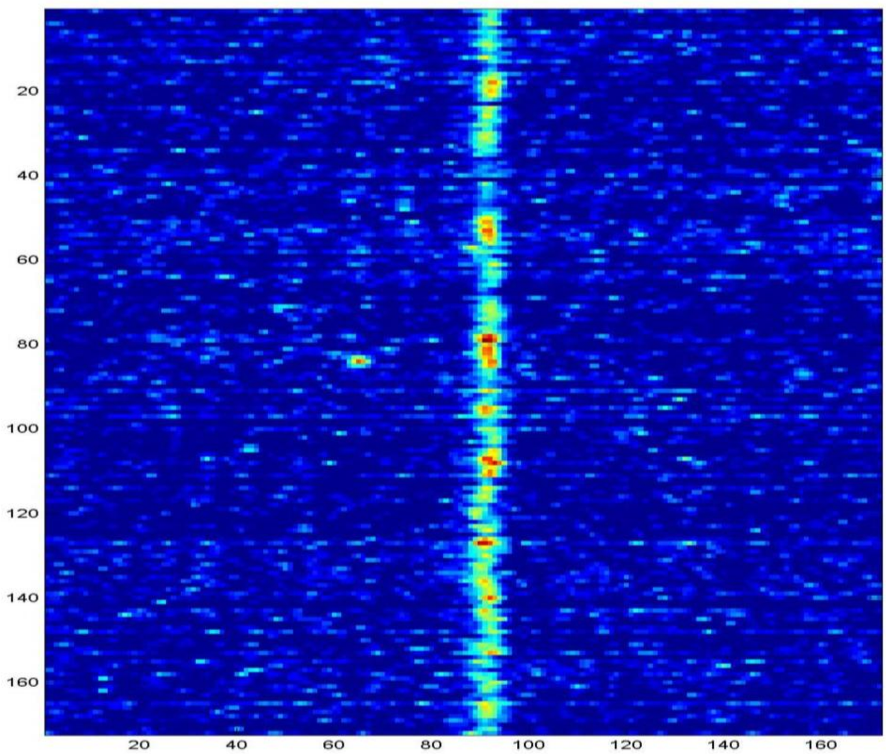

Gaussian fit of the pilot beam image projection with and without fixed pattern noise subtraction and corresponding raw image *Plot 3.9*

Comparison between reference Wire Scanner and IPM

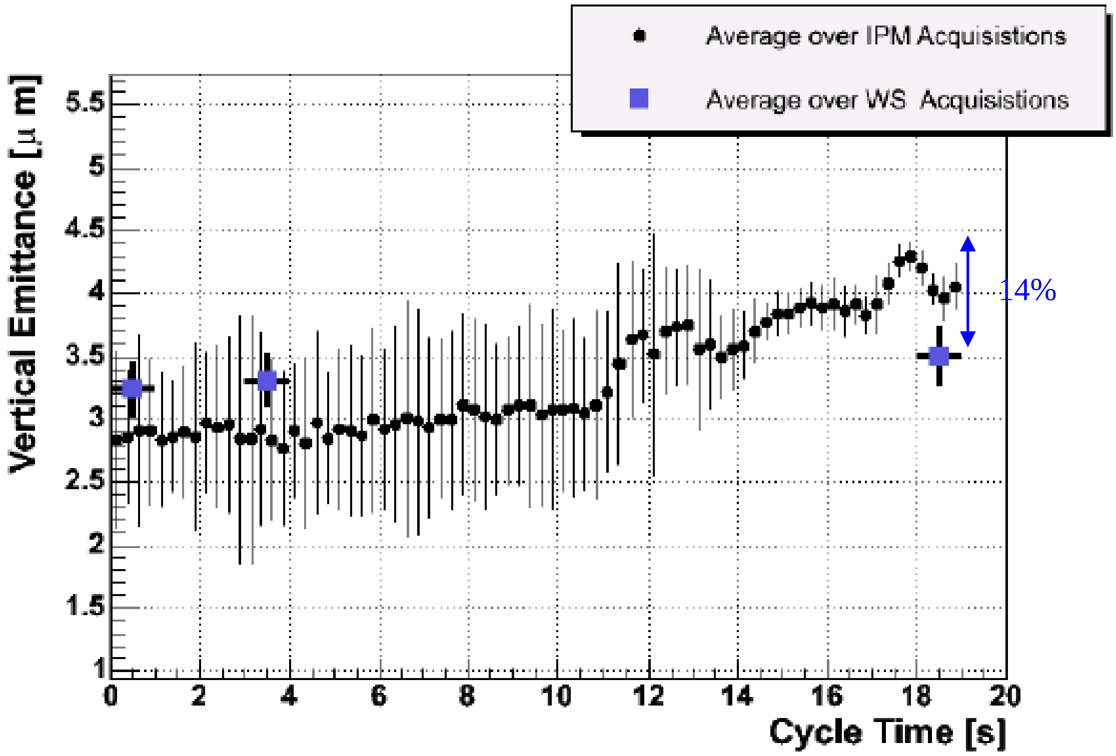

Comparison of the measured emittance between reference Wire Scanner and IPM with nominal LHC beam *Plot*

This particular data (**plot 3.10**) shows quite a good agreement between Wire Scanner and IPM. Maximum deviation was cca 14% at flattop and cca 10% at flat bottom. The WS is supposed as reference, because it is a mechanically simple and straightforward instrument. It is just a non-conductive wire in a large fork passing at high speed through the beam. Intensity of the scattered particles (detection by scintillators) is proportional to the beam profile.

On the **plot 3.11** (one acquisition from 3.12), the bunch spacing was 75 ns. With very low gain, we had quite a nice signal without any evidence of electron cloud. HV settings were (expectation): Cathode –1.2kV; MCP_{in} 1.2kV; MCP_{out} 1.8kV (or 1.85?); Phosphor 7.3kV. However, nobody knows, what was set inside the instrument, because the gain was progressively raised and an intensity drop appeared in between!

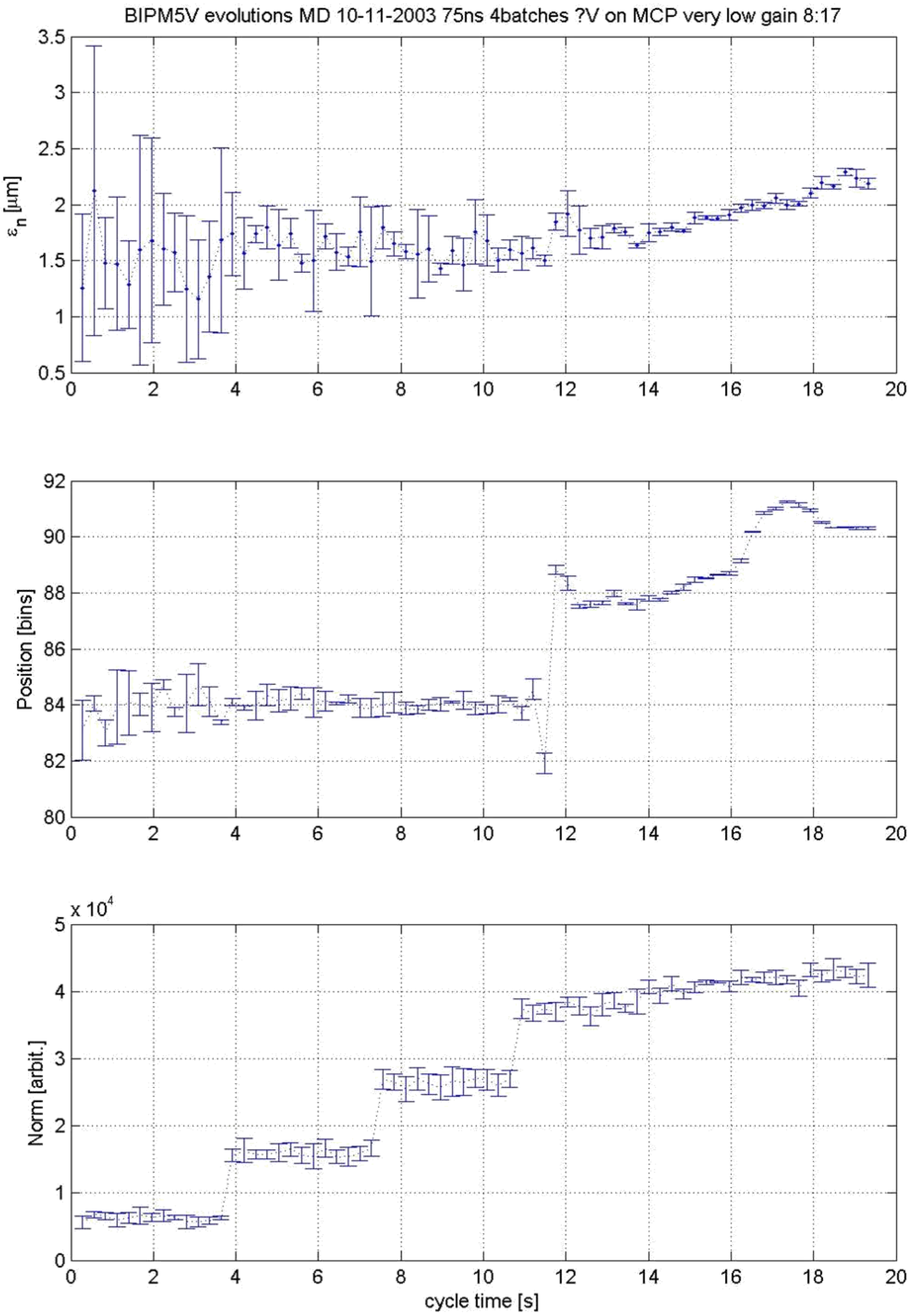

During a malfunction of the control program, the relative electron flux was surprisingly very stable (flat Norm) *Plot 3.11*

With some higher gains, there was a mysterious behavior (**Plot 3.12**) of the MCP discovered. Changes in norm level are due to differences in MCP gain level. The spikes could be caused by some MCP instabilities. Any beam instabilities are almost excluded, because the emittance is not changing during this phenomenon.

The emittance blowup at the end of acceleration could be due to limited bandwidth or beam bowed up itself.

The very small gain acquisitions were made with 1.95kV or 1.8kV (could be 1.85) set on the MCP_{out} (see 3.11). This could be a hardware program problem.

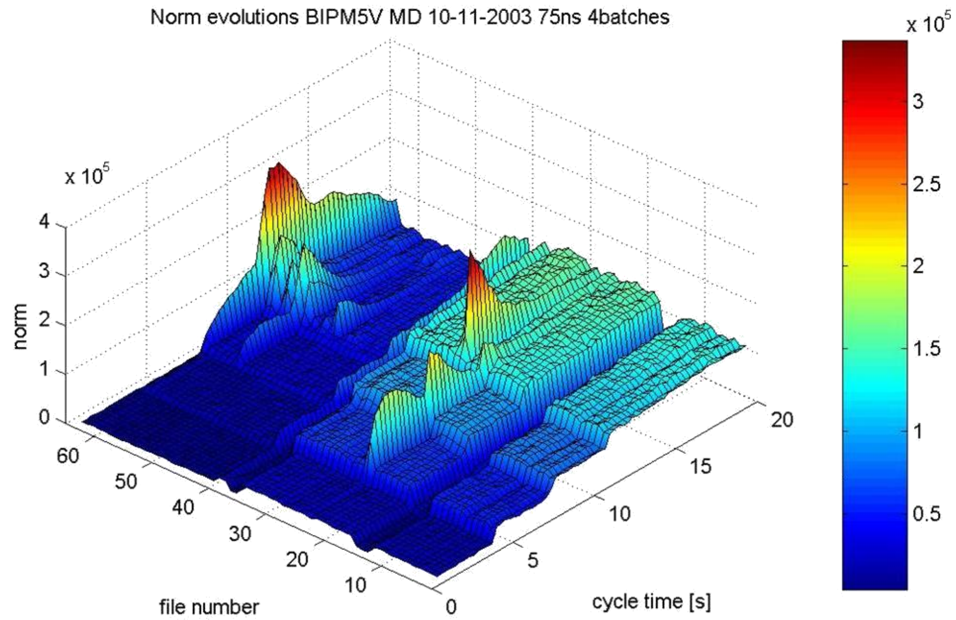

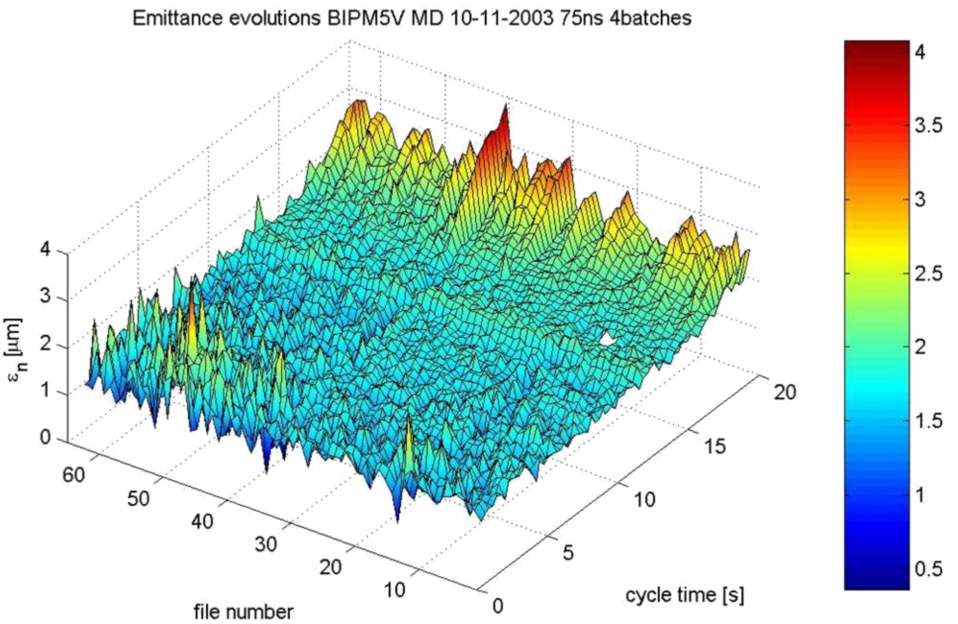

Important instabilities (peaks in norm) discovered in the MCP gain while the measured beam emittance was relatively stable *Plot 3.12*

Such a behavior was found also later (**Plot 3.13**) with only 2 batches injected, during the same MD. This time one instability is not starting at the injection point, as it was the case previously. This plot eliminated a possibility of a mismatched injection from PS causing this phenomenon.

Ideally (without particle losses and MCP saturation), the Norm should stay constant between two injections and during acceleration, because the signal from each particle stays constant. Only the space density changes with energy.

We suppose that the N_2 ionization cross-section is rather constant for protons in this energy region (*Fermi plateau* in the *Bethe-Bloch formula*).

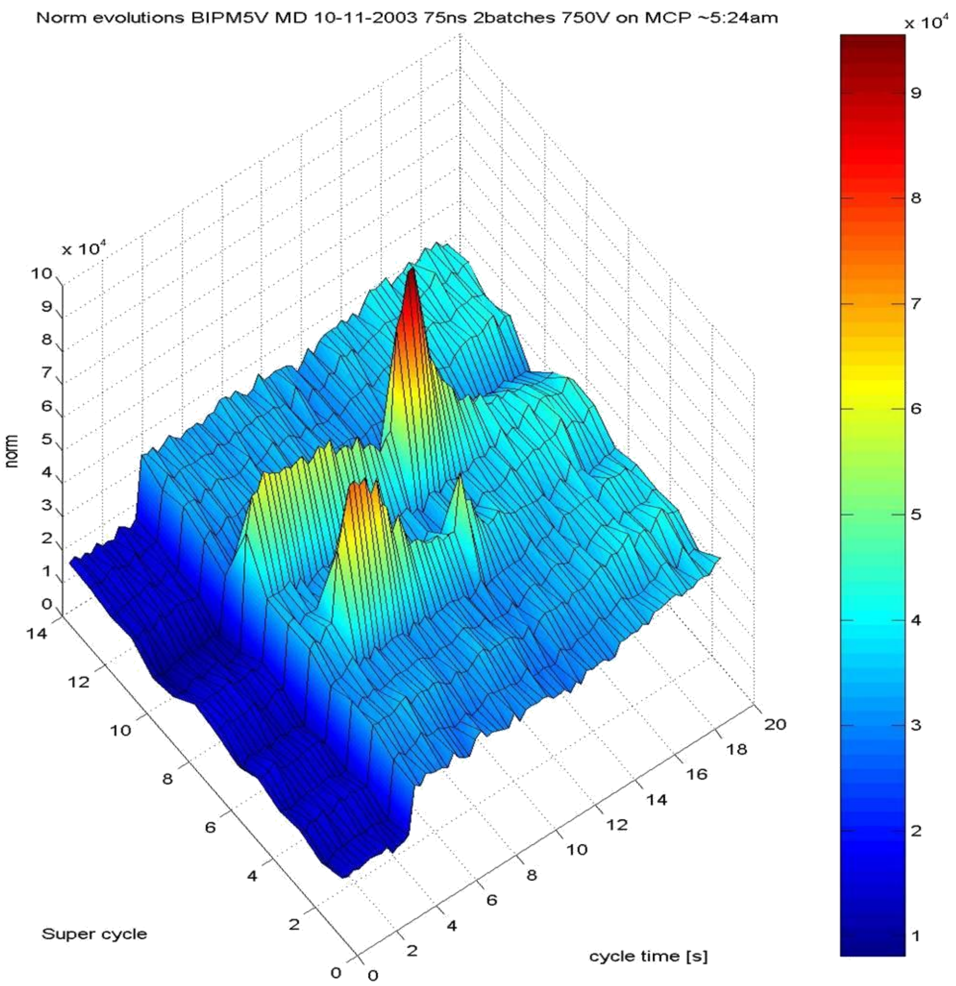

Observed instability does not start at injection *Plot 3.13* ·

The last beam in the SPS 2003 run was during the MD 11/11.

We have seen and measured the LHC type pilot bunch, normally used for injection matching studies because of its very low intensity (not damaging the accelerator installation). Plot 3.9 comes from this MD too. The relatively high noise is due to a high gain used on the MCP. The pilot bunch is supposed to be very stable (no collective instabilities, little induced EM fields etc…) so it can give a clear picture of the system's performance.

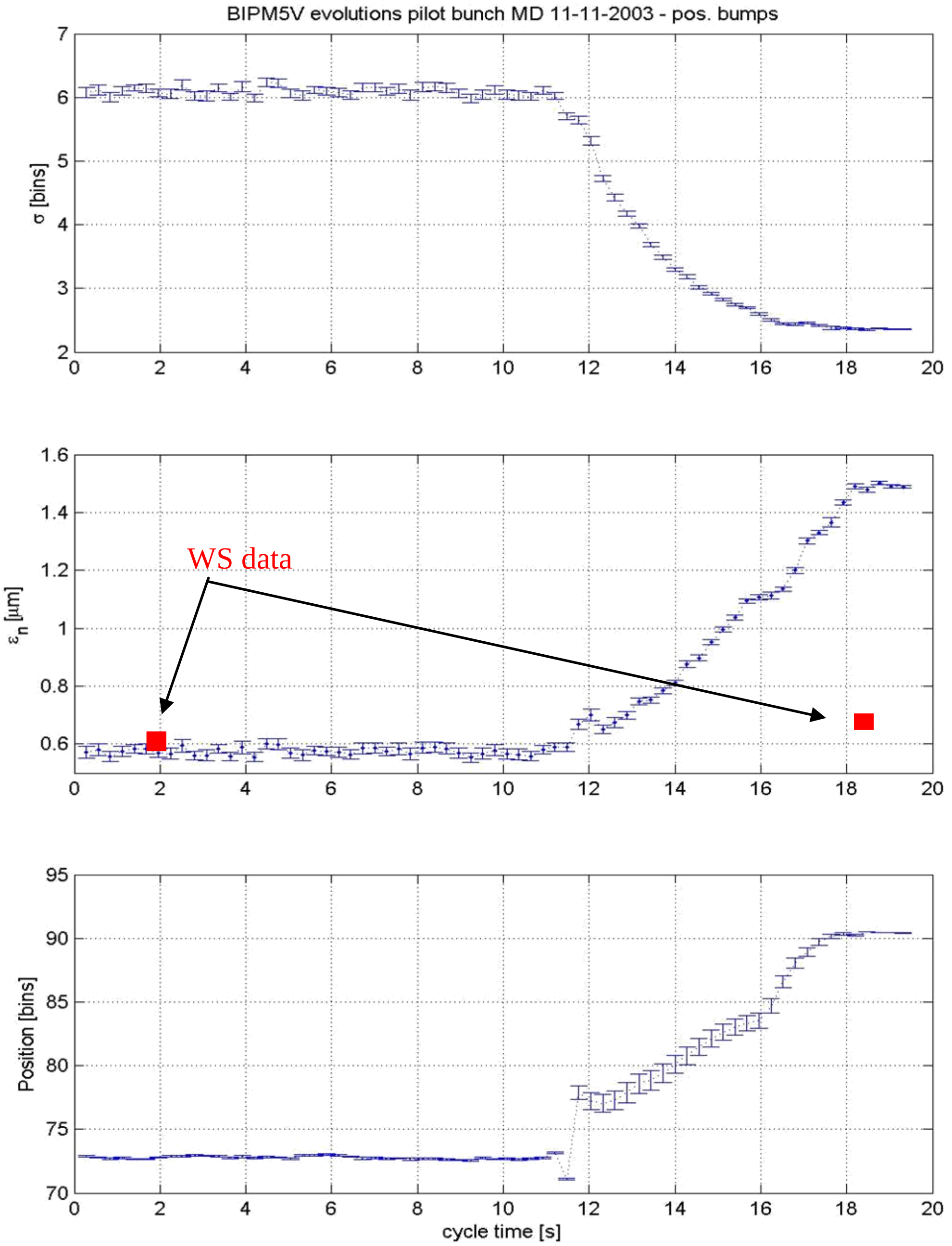

Pilot beam measurements with position bump showing resolution limits of IPM (compared to WS) and non-homogeneity of the MCP *Plot 3.14*

At the very end of the MD, a beam orbit was introduced in LSS5 vertical plane to have the beam image (as previously) in the not damaged region of the MCP.

We measured the smallest emittance (**Plot 3.14**) during that year. Wire scanner measurements were showing the normalized emittance around 0.6µm at the flat bottom and 0.65µm at the flattop. The agreement at 26GeV was excellent. Nevertheless, during acceleration the emittance was growing up to 1.5µm at 460GeV.
This is supposed to be caused by the limited bandwidth of the video acquisition card and the too small optical resolution. Moreover, there could be also a contribution from the orbit bump, which was not necessarily completely closed and might have caused a little beam blow-up.

Plot **3.15** shows for illustration one beam cycle acquisition of the Pilot bunch. The orbit bump completely vanishes for the last profiles, because the orbit correctors are not enough powerful to deviate the beam at 450GeV (beam gradually returns to its un-deviated orbit). One can clearly see the beam size shrinking during acceleration and the beam stability throughout the flat bottom.

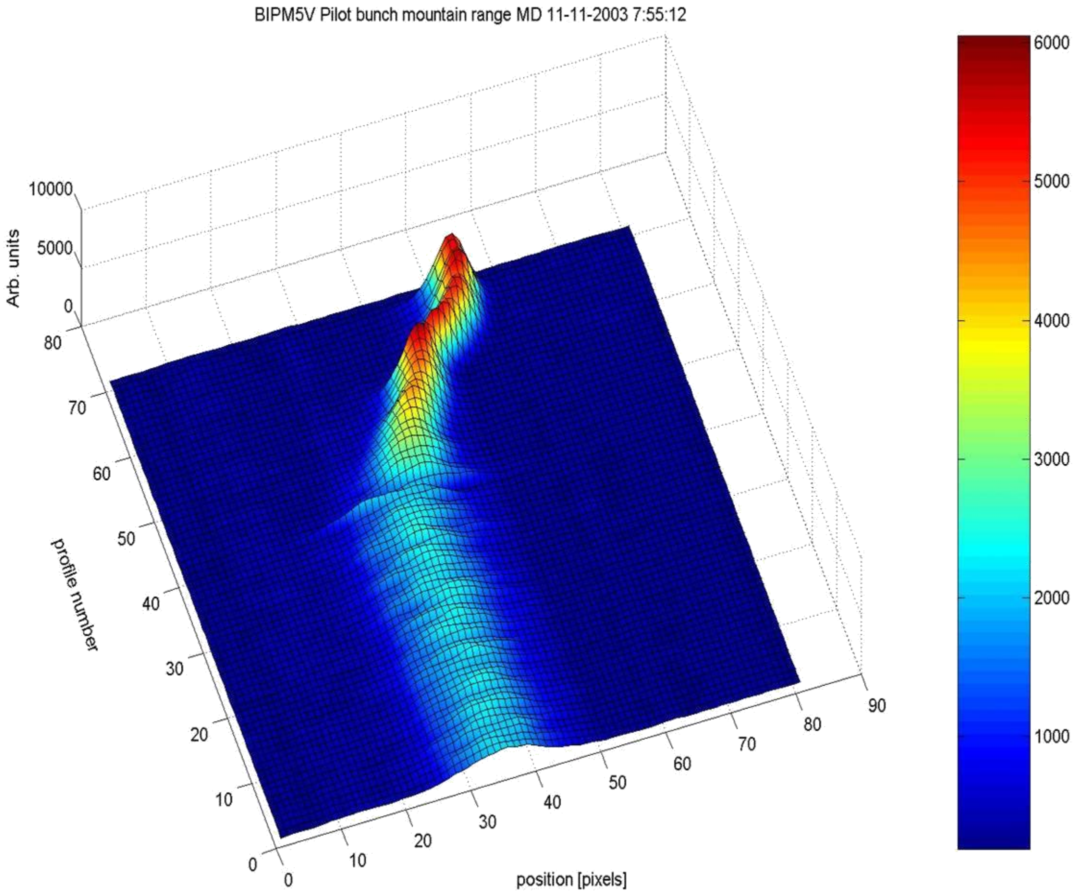

Profiles sequence during a complete acquisition with a position bump *Plot 3.15*

4. Optical design for IPM imaging system

4.1. Expected parameters

The optical system used during the 2003 run inside the BIPM5 in LSS5 consisted just from a fused silica prism (with the deposited phosphor layer serving as object), vacuum window of the tank and an intensified CCD camera with a C-mount 50/1.3 lens.
Reasons for developing a new optical system were mainly three.

- increase the resolution of the system (Target was 1% of relative error)
- add a second optical path for a fast low resolution detector (Multi Anode Photo Multiplier)
- increase the luminosity of the system

There were several constraints for the design. Diameter of the lenses was limited mainly by the hole in the IPM dipole magnet, though where the light path was leading. Maximal final diameter was chosen as 50.2mm. The overall system length was limited to approx. 70cm including camera body. Position of the light splitter was fixed. It was decided not to place any optics inside the vacuum tank, so there was a minimum distance of the first lens to the object.
The main parameter for the design was the paraxial magnification. It was calculated simply as *m = image size / object size*. Object size was the length of the phosphor screen and the image as the shortest side of the CCD elements used.
Two new CCD type sensors were considered. The EM CCD (Electron Multiplied CCD) and EB CCD (Electron Bombarded CCD). Both devices do not need any further light amplification. It was also decided to match the magnification to the shorter side of the larger CCD (EM) and to use the EB CCD tilted by 90° (see fig. 4.1).
Designed optics had to fit inside the C-mount system and have a reasonable cost.

Object size (Phosphor)	44 x **44**mm
EM CCD size	11.52 x **8.64**mm
EB CCD size (2/3’’)	8.8 x 6.6mm
Multi Anode PM (2nd path) size	32 x **32**
Paraxial magnification	0.196 (or smaller)
Paraxial magnification (Multi Anode PM)	0.7
Distance to the first lens	250mm
Minimum distance to detector	430mm

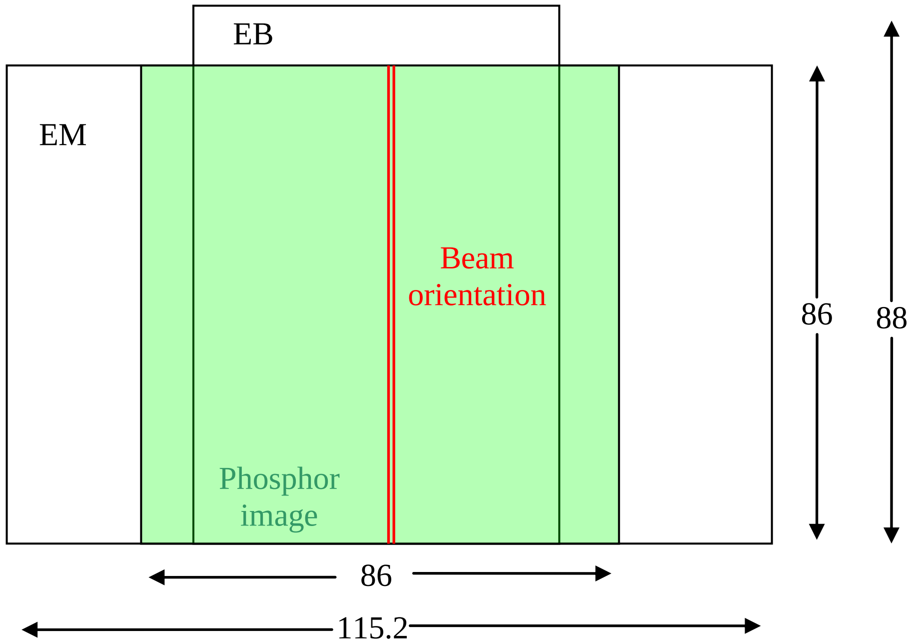

EM and EB CCD chip orientation and size *Figure 4.1*

4.2. Starting design for Zemax code optimization

Zemax code was chosen to perform the simulations of the design and its optimization. If one wants to make a good design in a reasonable time, he has either to have an important experience in the field either chooses a good starting design verified in the past (or both). Only the second variant was possible and after several (quite a lot...) attempts, a final concept was chosen.

Two commercially available doublets had to be placed between the vacuum window and the splitting prism with an aperture stop amid. Magnification of this part should be matched to the PM and no more lenses used after the splitter in the second path.

Between the splitter and the CCD in the first path, an objective should be placed to match the magnification to the EM CCD.

The Petzval 150 year old design with 2 positive power doublets was used as the starting point.

4.3. Optimization and Final design

Optimization of an optical design requires a merit function that incorporates the target values of the system. Major part of this function was generated by the program to optimize mainly on the rms spot size for the defined image points and a range of wavelengths 520 – 580nm with a maximum weight at 550nm. A higher number of dimensional constraints had to be carefully set and progressively modified with the optimization evolution. Without these, a system not realizable in the 3D space (or the budget space) would be produced (like interfering lenses etc…).

It is important to know whether the chosen glasses are in your producer's stock, if he can produce such diameters and radii and also if the design could be mechanically mounted in some support. Glass price is also crucial, because it can vary in several orders of magnitude. Focusing of the system should be possible.

During optimization, the first objective lens was found as not crucial for the performance and optimization continued with only three lenses. There were several attempts to substitute the designed lenses with some commercially available ones, but this degraded the system's performance too much.

The diameter and length of the last element was found as the major constraint, because it had to fit inside the C-mount and to be mechanically hooded outside it. Numerical aperture in the image plane had to be limited too, because the CCD elements do not accept rays at higher angles.

Usually the Global optimization was used to find a minimum of the merit function. Glass types were changed too. Afterwards, the powerful Hammer optimization was trying to escape from a local minimum using a different algorithm.

Figure **4.2** shows one of the last designs.

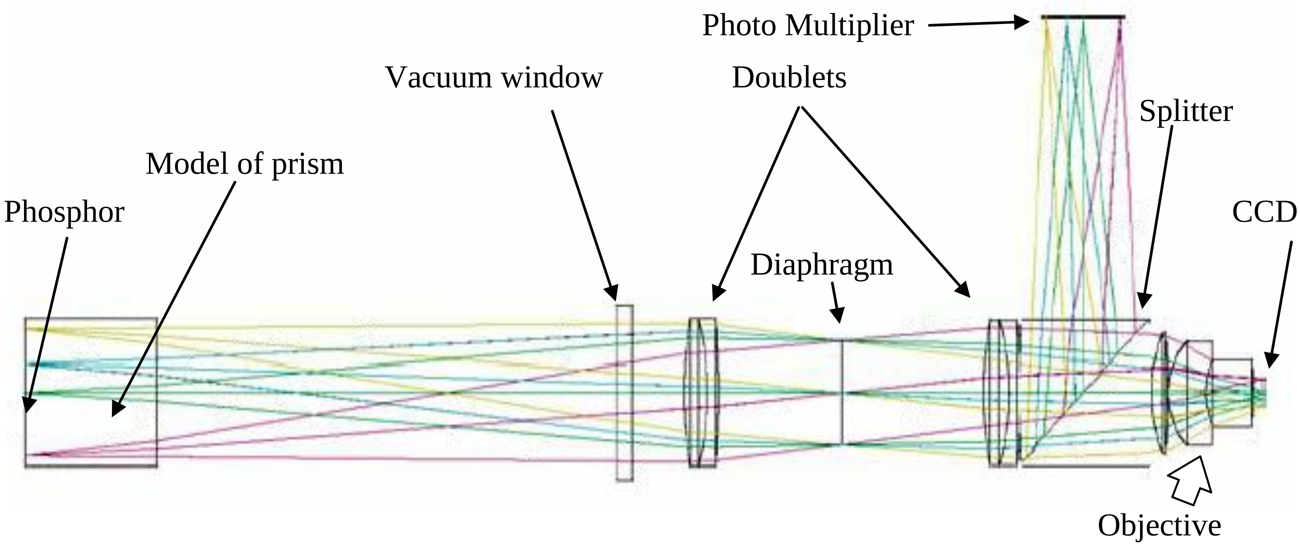

Description of the designed optical path with 2 detectors *Figure 4.2*

Because of mounting difficulties, the front surface of the last element (figure **4.3**) was fixed to be flat (R = ∞) without any important losses of image quality. The whole group had a possibility of focalization by its axial movement.

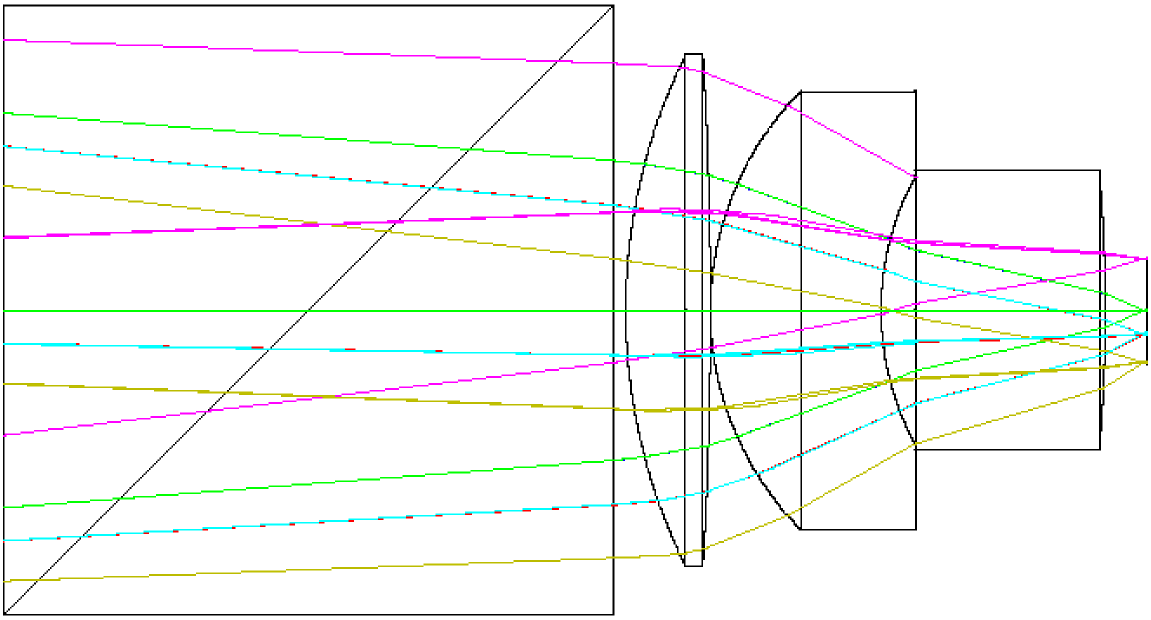

Detail of the 3-element objective following the splitter *Fig 4.3*

The final design consisted of two Optosigma© doublets (200.1 and 169.8mm focal length), a diaphragm almost in the middle of them and the tree element objective in one group. It was finally found that the chosen glass for the first element was not in the suppliers stock, so it was rapidly exchanged by another one, but also not in stock. Finally, it was found possible to use the first and second element with the same glass type.

The finally used materials were then SK16, SK16 and SF14.

Final design parameters (Zemax output)	
Effective Focal Length :	90.24992
Back Focal Length :	-13.63504
Total Track :	428.9591
Image Space F/# :	1.825016
Paraxial Working F/# :	1.220339
Working F/# :	1.247366
Image Space NA :	0.3791332
Object Space NA :	0.0784591
Stop Radius :	17.94123
Paraxial Image Height :	4.643525
Paraxial Magnification :	**-0.1921504**
Entrance Pupil Diameter :	49.45158
Entrance Pupil Position :	314.1709
Exit Pupil Diameter :	28.7407

Exit Pupil Position :	35.41758

The main merit target was in fact just the x component of the image spot; because mainly that one contributes to the resolution of the beam image (we are anyway summing the lines along the y coordinate). One can see (fig. **4.4**) that the achieved resolution (in the image space) was from 25µm in the image center to 37µm at the edge.

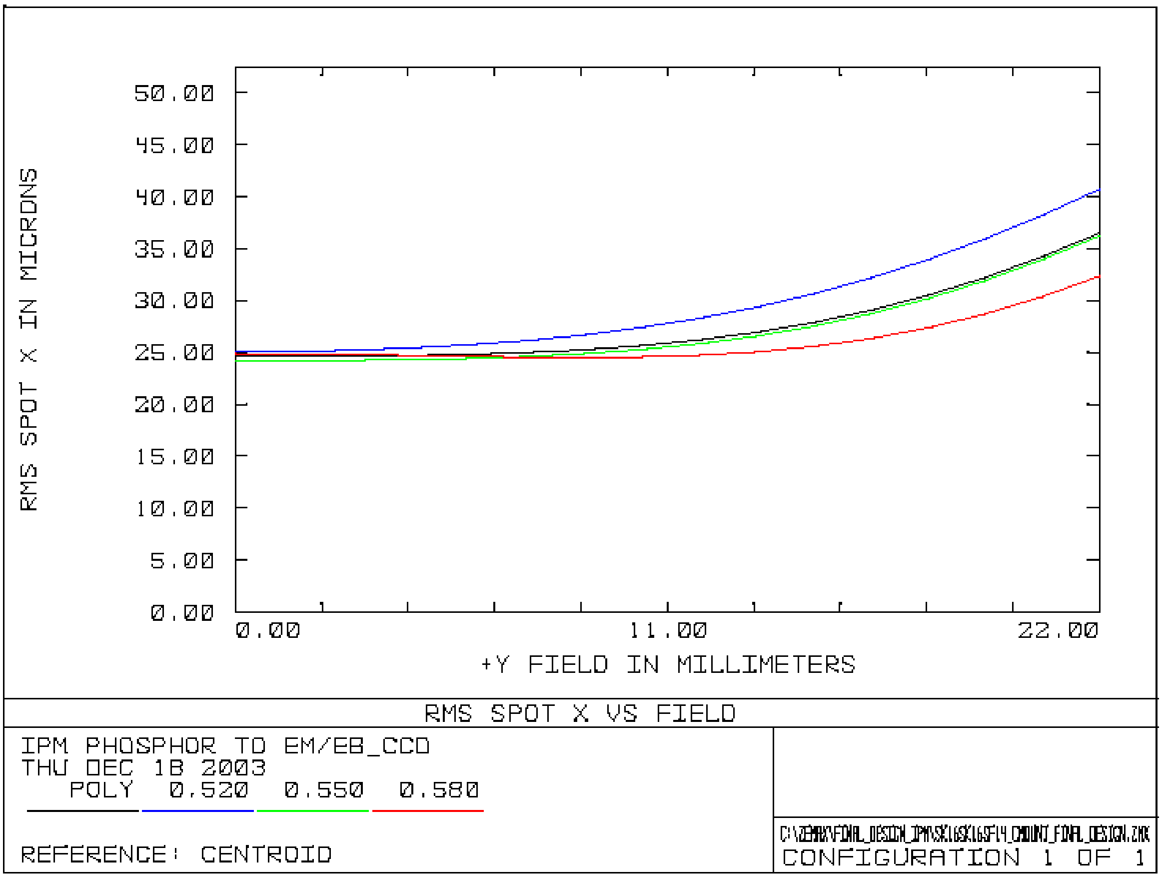

Transverse component of the RMS spot in image space (field in object space) Fig 4.4

Calculated systematic errors of the measured beam size		
Average beam size	**2.3mm (26GeV)**	**0.6mm (450GeV)**
Imaged size (IS) (mag = 0.191)	0.439mm	0.141mm
Max spot size (MS) (x axis)	37e-3mm	37e-3mm
Measured beam size $\sigma = (IS^2+MS^2)^{0.5}$	0.4406mm	0.1458mm
Relative error	**0.36%**	**3.3%**
Min spot size (mS) (x axis)	25e-3mm	25e-3mm
Measured beam size $\sigma = (IS^2+mS^2)^{0.5}$	0.4397mm	0.1432mm

Relative error	**0.16%**	**1.5%**

Geometrical distortion was also one of the merit function constraints, because it could contribute to the systematical error. One can see the maximum distortion of 2.4% at the very edge of the image. This seems too much but effectively the beam will never be in that region. Moreover, we would be interested just by its x-component and the error is a global one. With a small beam, the most important is the local error, which is negligible in this case.

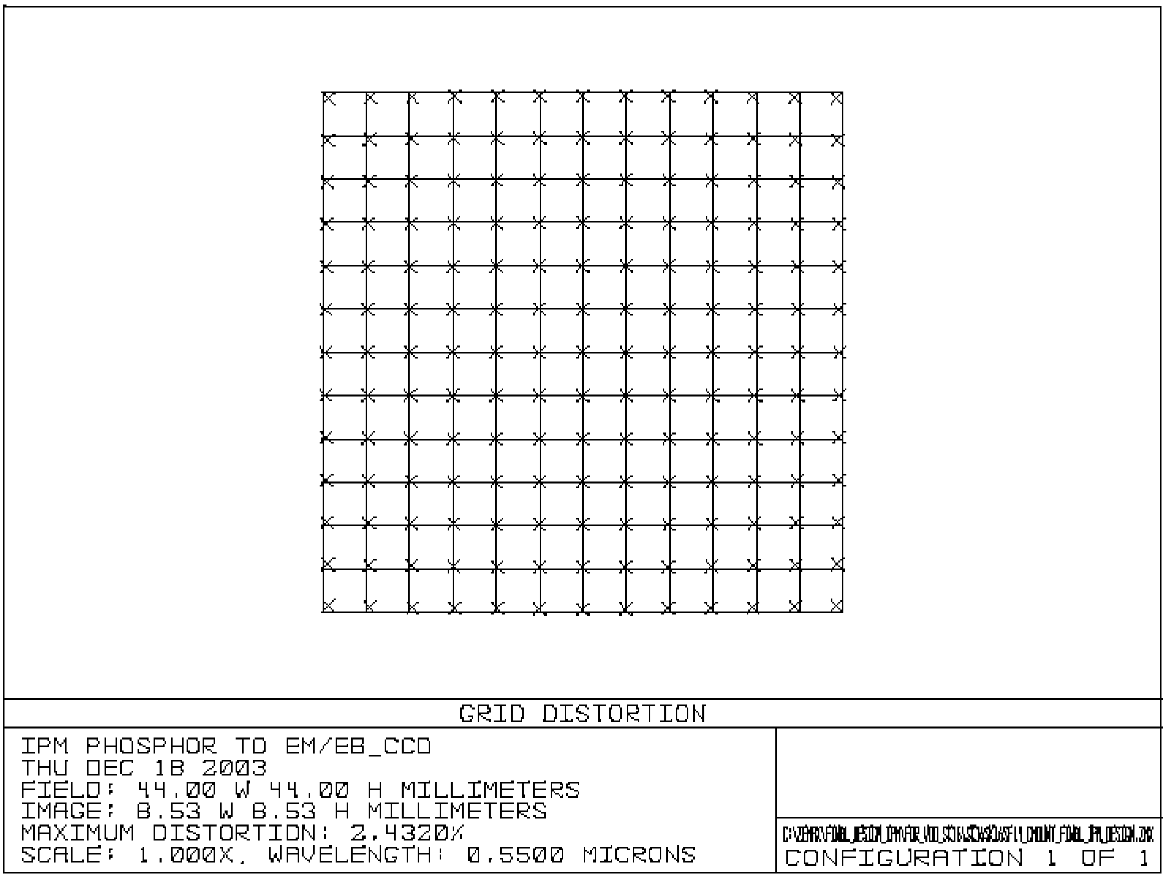

Geometrical distortion of a regular grid in the image space

5. Conclusion

It was demonstrated that the Ionization Profile Monitor was able to give solid and repeatable results in the full dynamic range of the accelerator energies. In addition, the beam currents from 1 pilot bunch to 4 nominal intensity batches (288 bunches) were covered. With the pilot bunch at high energy, there was however, a serious problem with optical resolution combined with the small bandwidth of the acquisition card and maybe other factors too. The electron cloud problem was still present during 25ns bunch spaced beam, but has almost disappeared for the 75ns spacing.

Later, when the monitor's performance will be upgraded it might be important to verify its sensitivity to the momentum dispersion. In addition, one should compare the Fixed target behavior and the LHC type beam.

We have introduced an almost automatic offline analysis (via Matlab files) of the data from IPM and contributed to the upgrades of the instrument throughout the year.

The optical design was made after a major effort, satisfying the expected parameters almost completely. Two doublets were sent by the supplier and the three designed lenses were produced in Vývojová Optická Dílna in Turnov (Academy of science, CR). The system was mounted together, but the detector has already been inside the tunnel so it could not be installed so far.

I would like to thank to my former colleagues Bernd Dehning, Jan Koopman and Federico Roncarolo for their great support and help during my stay in CERN and to my supervisor from the Technical University of Liberec, Miroslav Sulc for his remarks and support.

6. Bibliography

- Helmut Wiedemann (2003): Particle Accelerator Physics I, II (Springer-Verlag, Berlin Heidelberg)
- Stanley Humphries, Jr. (1999): Principles of Charged Particle Acceleration (Albuquerque, New Mexico)
- Rende Steerenberg (2003): AXEL introduction AB/OP CERN
- B.Dehning, C.Fisher, J.Koopman, D.Kramer, F.Roncarolo (2004): Continuous profile measurementsn the SPS: where do we stand?
- Jan Koopman (2004): IPM51734 Problems and Cures

7. Attachments

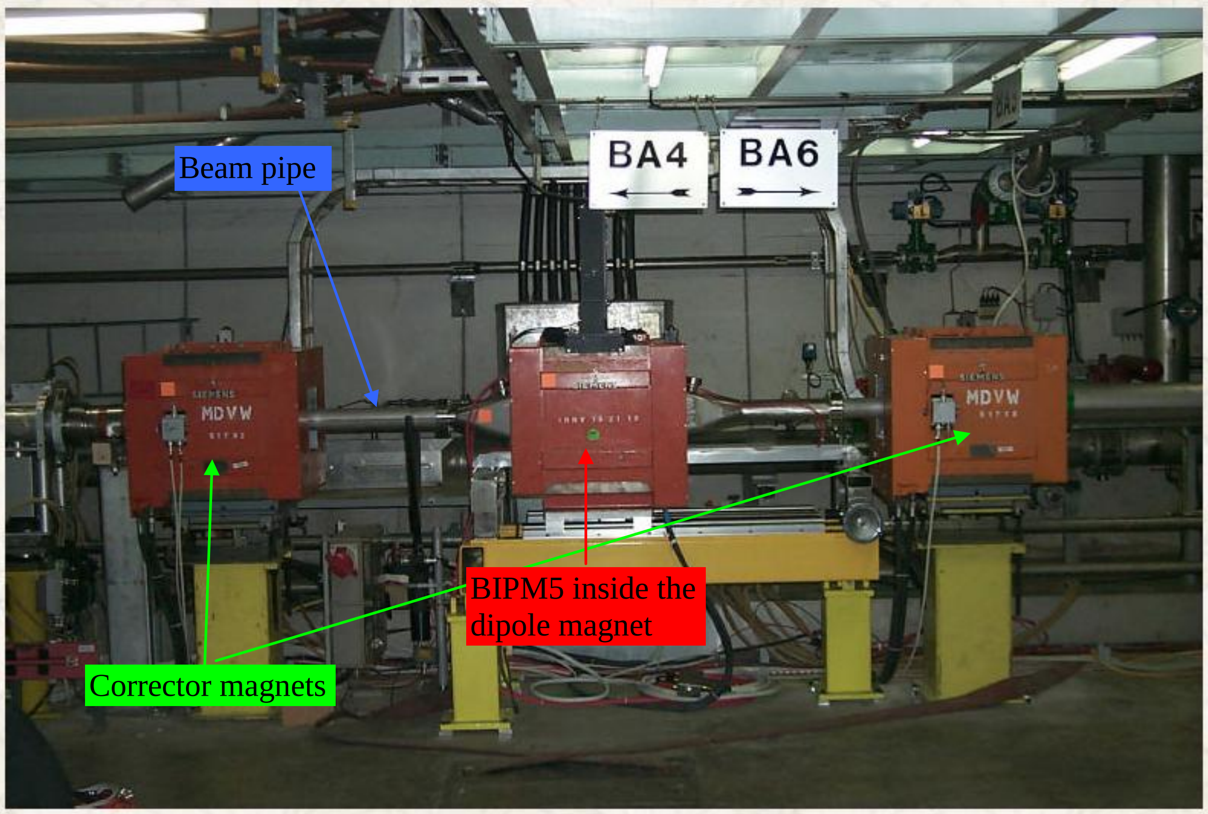

IPM detector and 2 magnet correctors photo in the underground SPS tunnel in LSS5

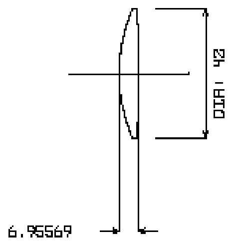

DIMENSIONS IN MILLIMETERS

LEFT SURFACE	MATERIAL	RIGHT SURFACE
R = 47.2355	GLASS: SK16	R = -349.827
	N_D= 1.620410	
	V_D= 60.32	
DIA$_d$= 42	THIC = 6.96669	DIA$_d$= 43
3/	0/	3/
4/	1/	4/
5/	2/	5/
6/		6/

ISO drawing of the front SK16 objective lens

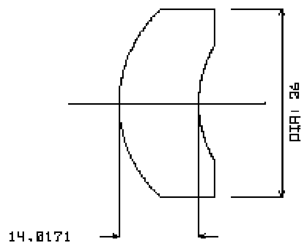

DIMENSIONS IN MILLIMETERS

LEFT SURFACE	MATERIAL	RIGHT SURFACE
R = 25.5491	GLASS: SK16	R = 23.1096
	N_D= 1.620410	
	V_D= 60.32	
DIA$_d$= 36	THIC = 14.0171	DIA$_d$= 32
3/	0/	3/
4/	1/	4/
5/	2/	5/
6/		6/

ISO drawing of the middle SK16 objective lens

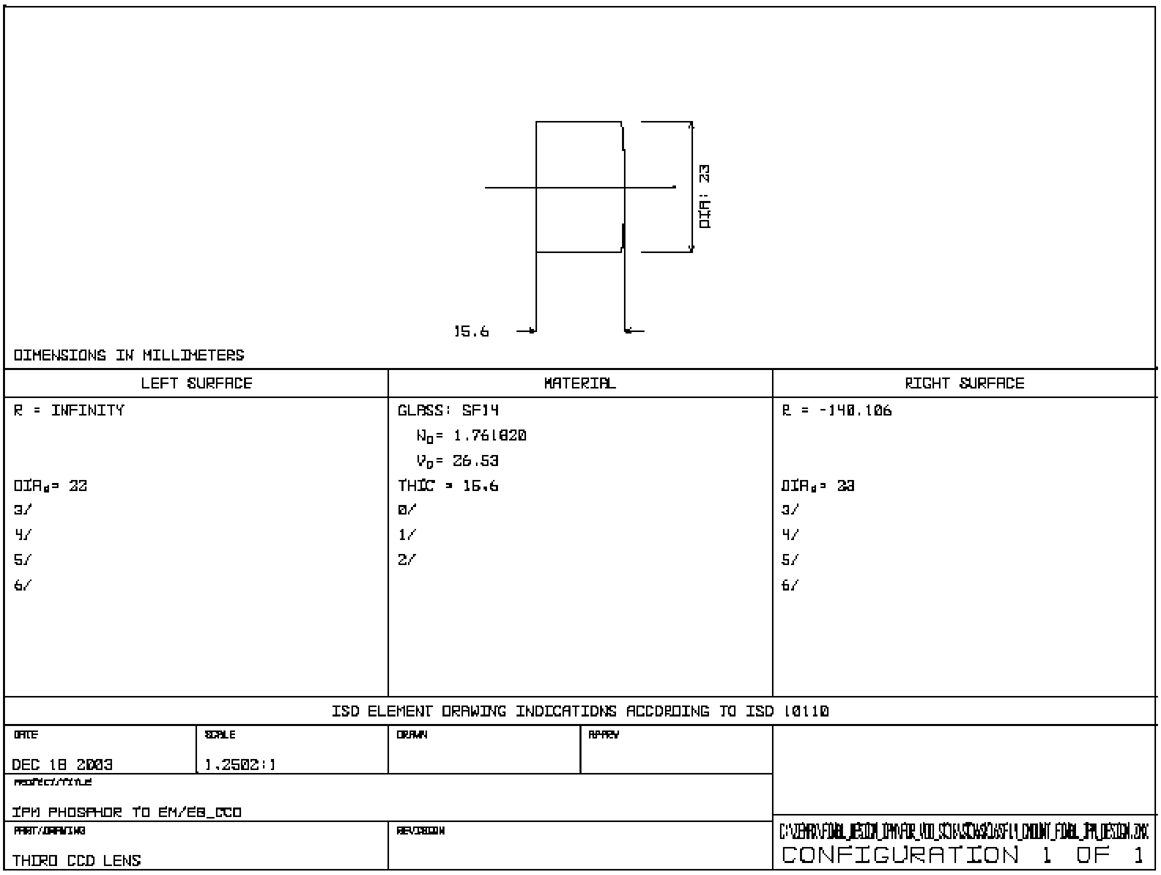

ISO drawing of the last SF14 objective lens

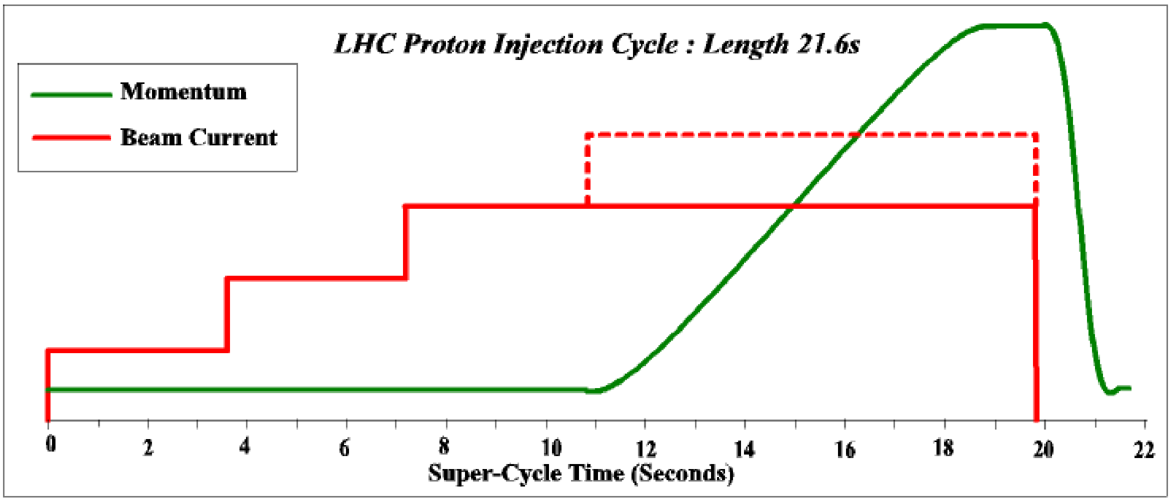

Standard SPS proton cycle used with LHC type beam, acceleration starts at 11s

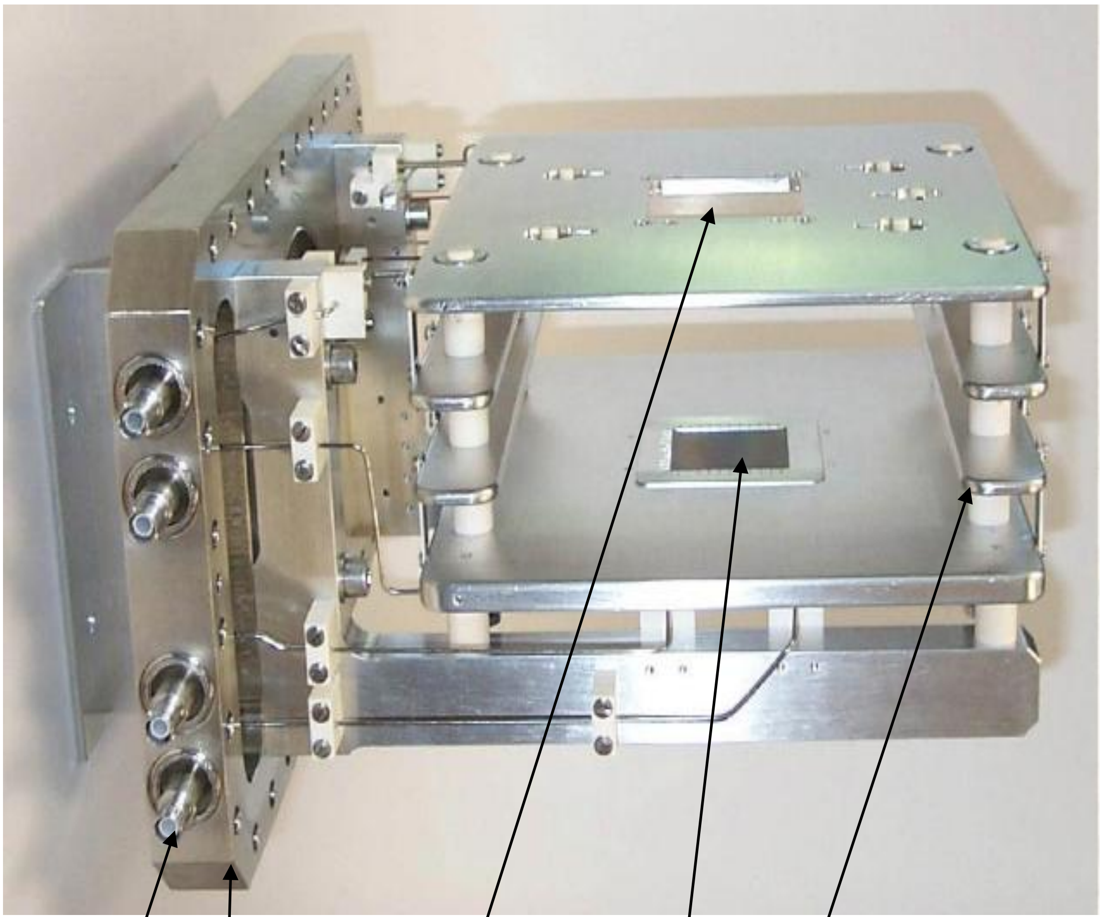

Detail of the interior part of the IPM

High voltage connectors

Vacuum tank lid

Cathode grid…………………..

Multi-Channel Plate (MCP_{in}) entrance electrode….

Field homogenization electrodes……………………..

SPS General Parameter List for LHC

	Units	SPS	
Momentum, p	**GeV/c**	**26**	**450**
Machine Radius, R	**m**	**1100**	
Minimum Vacuum Pipe Radius, b	**mm**	**25**	
Revolution time/frequency, T/f_{rev}	**μs/kHz**	**23/43.3**	
Betatron Tunes, Q_h, Q_v		**26.7**	
Gamma Transition, γ_t		**23.23**	
Maximum Number of bunches, k		**288 (4*72)**	
Intensity per bunch (nominal/ultimate)	**10^{+11}**	**1.1/1.7**	
Maximum Total Intensity (nominal/ultimate)	**Ampere**	**0.22/0.34**	
Bunch Spacing, s	**ns**	**25**	
Bunch Frequency, f_b	**MHz**	**40**	
(Full) Bunch Length, τ_t/τ_s	**ns/mm**	**4/1200**	**1.74/520**
Peak intensity, (ultimate)	**Ampere**	**10.9**	**25**
Transverse Normalized Emittance, ε	**μm**	**3.0**	**3.5**
Average Beam Size, σ	**mm**	**2.3**	**0.6**
Longitudinal Emittance	**eVs**	**0.35**	**0.5-1.0**
(Main) RF Frequency	**MHz**	**200**	